2

A Close-Packed-Carbon-Nanotube Film on SiC for Thermal Interface Material Applications

Wataru Norimatsu[1], Chihiro Kawai[2] and Michiko Kusunoki[3]
[1]*Graduate School of Engineering, Nagoya University*
[2]*Electronics & Materials R & D Laboratories, Sumitomo Electric Industries, Ltd.*
[3]*EcoTopia Science Institute, Nagoya University*
Japan

1. Introduction

Carbon nanotubes (CNT) are predicted to have an extremely high thermal conductivity along the tube axis of 6600 W/mK (Berber, 2000) while experimental results (Fujii et al., 2005; Kim et al., 2001) have produced values of 2000~3000 W/mK. However, only a few studies have investigated CNTs for use as thermal interface materials (TIMs) (Biercuk et al., 2002; Liu et al., 2004; Huang et al., 2005). In this study, we focus on the heat-release structure of a central processing unit (CPU). Figure 1 shows the schematic diagram of the typical heat-release structure.

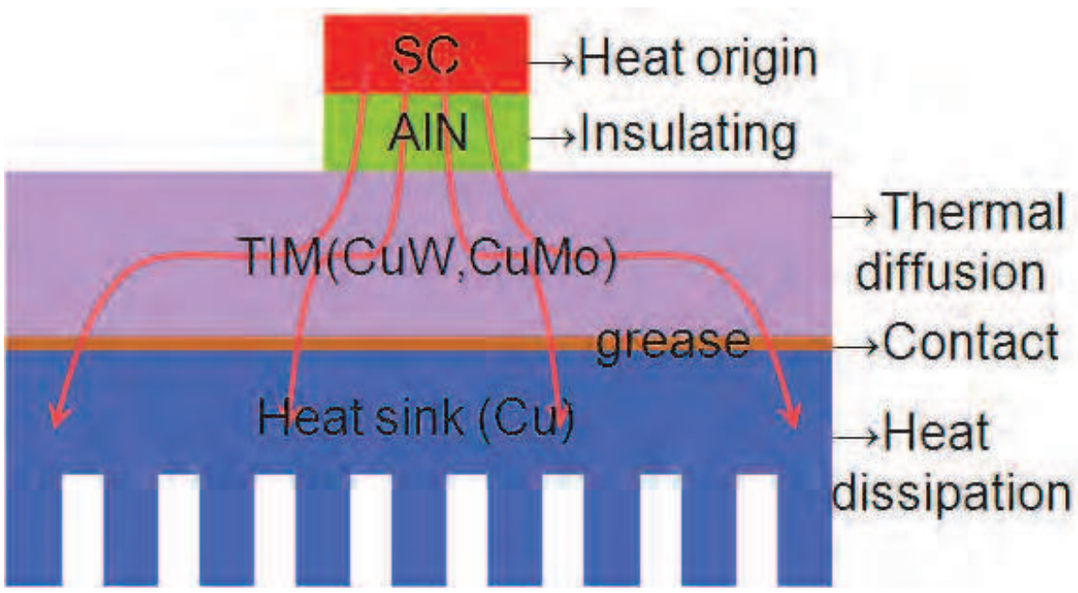

Fig. 1. Schematic diagram of the typical heat-release structure.

In the typical structure, TIMs such as Cu-W alloys, Cu-Mo alloys, Al-SiC solid solution and so on, are used to dissipate heat efficiently from the heat source, such as a semiconductor (SC), to heat sinks. Recently, a rapid increase in the heat generated by various electronic

devices requires an urgent development of high-performance TIMs. The performance of the actual TIMs depends not only intrinsic thermal conductivity, but also on the thermal resistance. Here, the thermal resistance of TIMs is given by the sum of their intrinsic thermal resistance and the contact thermal resistance between the TIM and the contacting material. It is thus important for thermal management to reduce the contact resistance on the contact face as well as to employ highly thermal conductive materials. Actually, in order to reduce the contact resistance, a layer of grease ranging from 50 to 100 μm thick is applied to the contact face between the TIM and the contacted material. The grease intrudes into the microscopic undulations and surface roughnesses of the contacted material, and eliminates any air gap, leading to an increase of the contacted area and a consequent decrease of the contact thermal resistance. However, the total thermal resistance does not decrease efficiently with the use of such a thick grease layer, since the intrinsic thermal conductivity of grease is low.

To reduce the total thermal resistance, thermally conducting AlN or Ag particles are dispersed into the grease, but they lead to higher costs and the thermal conducting paths are interrupted in the particle-dispersed structure. On the basis of the high thermal conductivity of CNTs, some investigators have investigated various uses of to reduce total resistance; dispersing CNTs into plastics or embedding an aligned CNT array in a silicone elastomer, resulting in thermal conductivity enhancement (Biercuk et al., 2002; Liu et al, 2004; Huang; 2005). However, it is difficult to ensure a continuous thermal conducting path in the dispersed materials, and in the aligned materials, the low CNT density limits the overall heat conductance, the total thermal conductivity in these structures is reduced to the order of 1 W/mK. That is, workers have not succeeded in utilizing the extremely high thermal conductivity of CNTs.

2. Features of CNT/SiC composite material

We have reported that a vertically-aligned CNT film can be formed on SiC by a surface decomposition method (Kusunoki at al., 1997; 1999; 2000; 2002; 2005). Figure 2 shows the transmission electron microscope (TEM) image of the CNT/SiC composite material.

The features of CNT/SiC composite obtained by this method are,

1. high-density, well-aligned, and catalyst-free,
2. flexible CNT tips (Miyake et al., 2007) ,
3. high thermal conductivity of SiC (Burgemeister et al., 1979) and the CNTs, and
4. high adhesive strength of CNTs with the SiC substrate.

In other words, a CNT/SiC composite material meets the requirements for TIMs. In this study, then, we investigate the heat transfer characteristics of CNT/SiC composite materials made by the surface decomposition of SiC.

The CNT/SiC composite materials were prepared by the following procedure. A 6H-SiC single-crystal substrate and a polycrystalline SiC substrate obtained by the CVD method were cut into 10 × 10 × 0.25 mm^3 pieces, and their both sides of surface were polished. Carbon nanotube films with thicknesses of 1 and 4 μm were formed on the two sides of the SiC substrate by heating the substrate in a vacuum of about 10^{-4} Torr at temperatures of 1700 and 1900 °C, respectively. Observations of the microstructure of the CNT/SiC composites were carried out using a scanning electron microscope (SEM) and a JEM-2010-type transmission electron microscope (TEM).

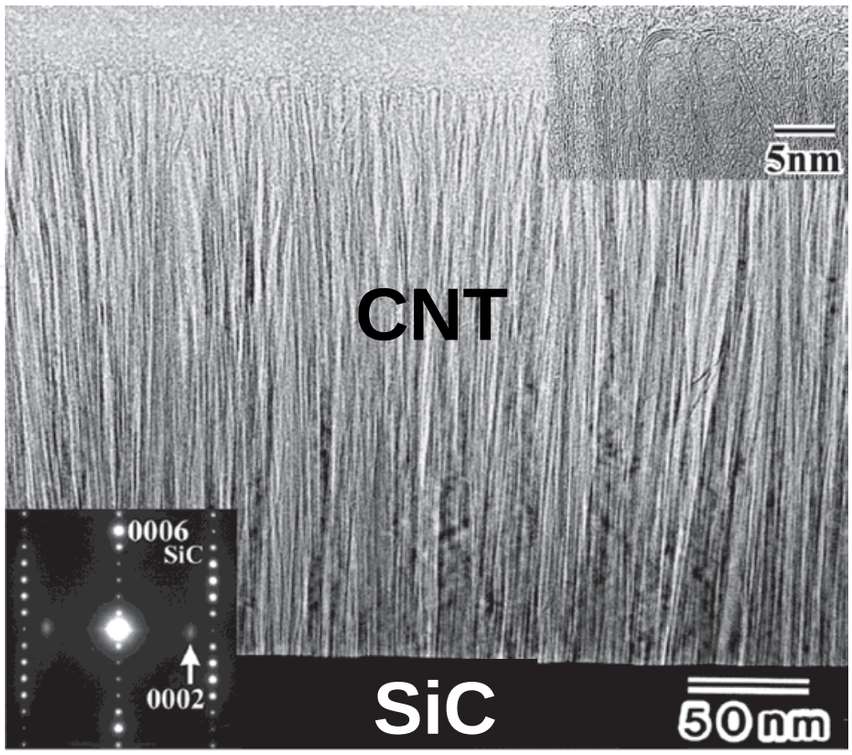

Fig. 2. TEM image and the corresponding electron diffraction pattern of CNT/SiC composite. High-magnification image around the CNT cap is inserted.

3. Thermal transport properties of CNT/SiC composite materials

Thermal resistance measurements were performed using an apparatus based on the American Society of Testing Materials (ASTM) Method D5470. A schematic diagram of the measurement system is shown in Fig. 3.

The prepared CNT/SiC composite material was sandwiched between three types of copper holders and a load ranging from 750 to 3750 g/cm^2 was applied from above. The surfaces of the copper holders were (1) R_z = 0.03 μm, and the flatness is ± 0.3 μm in 10 × 10 mm^2, (2) R_z = 1.0 μm, and the flatness of ± 0.3 μm, and (3) R_z = 1.0 μm, and the flatness of ± 15 μm. The upper holder was heated by a ceramic heater. Thermocouples were inserted in copper holders, and the temperatures at different positions were measured as shown in the right side of the Figure. The temperatures T_h, at the top, and T_c at the bottom of the sample, were obtained by extrapolating the temperature gradient. The thermal resistance R_t is given by the following equation, where Q is the supplied heat value.

$$R_t = (T_h - T_c) / Q \quad [\mathrm{K/W}] \tag{1}$$

For comparison, the thermal resistances of 100 μm thick samples of commercial silicone grease (G747, Shin-Etsu Chemical Co., Ltd., thermal conductivity of 1.09 W/mK) and grease with Ag particles (GR-SG014, TIMELY Co. Ltd., thermal conductivity of 9.0 W/mK) applied to the holders were also measured.

Figure 4(a) and (b) show, respectively, the SEM image of the CNT tips and the TEM image of the interface between the CNT and the SiC.

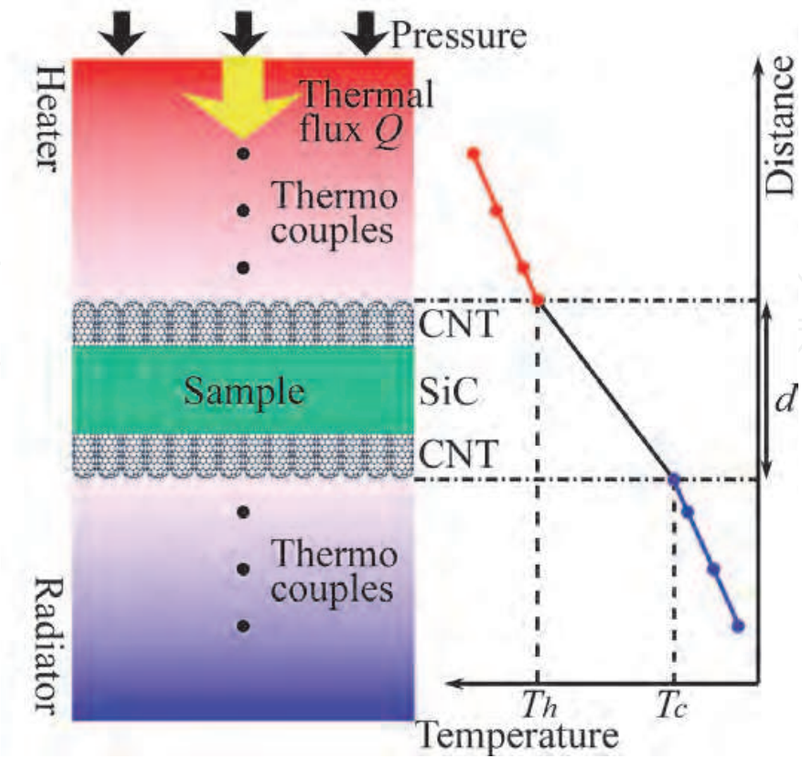

Fig. 3. Schematic diagram of the thermal resistance measurement system.

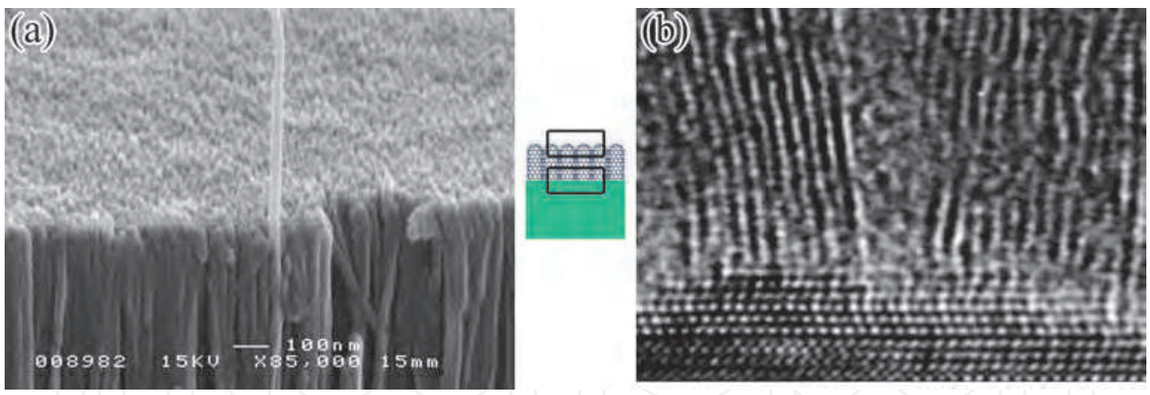

Fig. 4. (a) Scanning electron microscope image of the CNT tips. (b) High-resolution transmission electron microscope image showing the interface between the CNT and SiC.

As is seen in Fig. 4(a), aligned CNT bundles with a diameter of about 30 nm are closely packed and well aligned. We have reported that the planar density of CNTs obtained by surface decomposition of SiC is estimated to be about 3×10^4 μm^{-2} (Kusunoki et al., 1997). This density is more than one hundred times as high as that of CNTs grown by conventional CVD method (Lee et al., 1999; Pan et al., 1999). The high-resolution TEM image shows the presence of $(0002)_{graphite}$ lattice fringes almost perpendicular to the SiC surface. These fringes correspond to the walls of multiwalled nanotubes. This image demonstrates that CNTs are strongly adhered to the SiC substrate at the atomic scale. Another feature of our

CNTs is the absence of catalyst and amorphous layers. We therefore expected that the thermal interface resistance between CNTs and SiC will be sufficiently low to be useful.
In Fig. 5, the thermal resistances of different samples are shown for an applied pressure in this case fixed at 3750 g/cm^2, with the flattest sample holder (1).

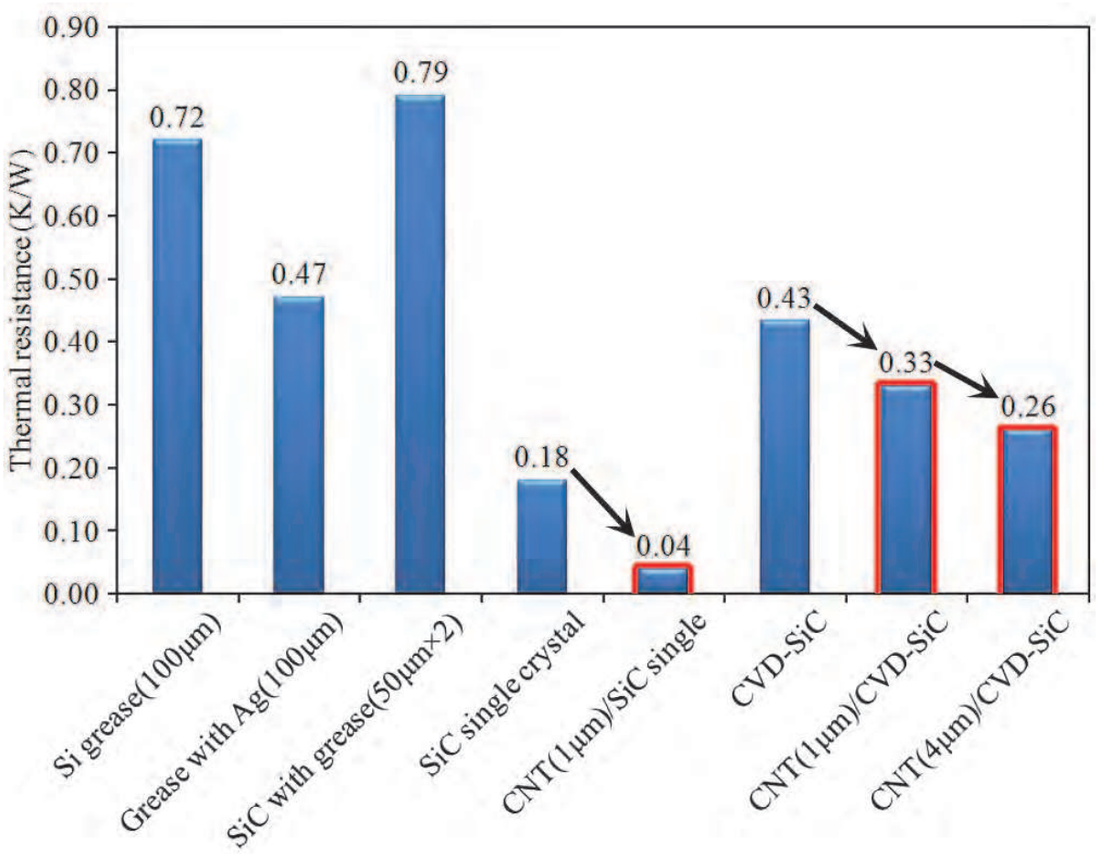

Fig. 5. Thermal resistances of various samples. Results obtained from the samples with CNTs are emphasized by the red lines.

The thermal resistances of silicon grease and grease with Ag particles were 0.72 and 0.47 K/W, respectively. The resistance of the pristine SiC single crystal was 0.18 K/W, reflecting the high thermal conductivity of the SiC crystal. The low resistance of pristine SiC indicates the high potential of SiC crystal itself as a TIM. It should be mentioned here that the intrinsic thermal conductivity of SiC crystal is about 360 W/mK, which is comparable to that of copper (403 W/mK) or silver (428 W/mK) (Burgemeister et al., 1979). In order to make a comparison practical TIMs, then, we measured the thermal resistance of the pristine SiC single crystal coated with silicon grease to a thickness of 50 μm. The result obtained was 0.79 K/W. This increase is attributed to the thick coating of grease. On the other hand, the thermal resistance of the 1μm-CNT/SiC single crystal sample was 0.04 K/W, which is a remarkably low value. This observation suggests that the contact resistance is drastically reduced by the use of CNTs instead of grease.
The thermal resistances of a polycrystalline SiC substrate produced by the CVD method (CVD-SiC), 1μm-CNT/CVD-SiC, and 4μm-CNT/CVD-SiC were 0.43, 0.33, and 0.26 K/W,

respectively. These results indicate that the resistance of CVD-SiC is higher than that of single crystal SiC because of the thermal scattering due to the presence of grain boundaries, but the resistance can be reduced by forming CNTs. We then concluded that CNT formation on both single-crystal and polycrystalline SiC can result in a high performance TIM.

As was mentioned above, it is important for thermal management to reduce the contact thermal resistance as well as adopting the use of thermal conductive materials. The thermal resistance values of CNT/SiC composites containing the contact resistance were quite low, which arises from the large contact area between CNTs and the contacted materials. We then altered the contact conditions by applying a load to the contact face, and remeasured their thermal resistance values. Figure 6(a) shows the pressure dependence of thermal resistance using the 1μm-CNT/SiC single crystal sample.

The resistance value rapidly decreases with increasing pressure, reaching saturation above 3750 g/cm^2. This result indicates that an increase of the pressure leads to an increase of the contact area. Schematic diagrams of the contacting conditions in the cases of low and high pressures are shown in Fig. 6(b). When the pressure is low, point contacts between the CNT tips and the contacted material raise the contact thermal resistance. At a high pressure, the flexibility of the CNT tips can lead to an increase of the contact area, which lowers the contact resistance drastically. Similar flexible buckling phenomena of these CNTs were previously reported (Miyake et al., 2007). When further pressure is applied, the contact area does not increase, giving rise to the saturation behavior above 3750 g/cm^2. In addition, it is quite important for the application that CNTs have never been peeled off from the SiC substrate during iterations of loading and unloading under such condition.

We here attempt the conversion of the measured thermal resistance into the thermal conductivity k in order to compare with the previous reports on TIMs. The measured thermal resistance R_t is given by the sum of the intrinsic thermal conductivity component d/k and the contact thermal resistance $R_{contact}$.

$$R_t \cdot A\ [m^2W/K] = d/k + R_{contact} \tag{2}$$

Here, d is the thickness of the sample, and A is the sectional-area of the sample. The intrinsic thermal conductivity is then given by the inverse of the gradient of the thickness-resistance graph, while the contact thermal resistance is given by the intercept of the same graph. Therefore, we should obtain both the intrinsic thermal conductivity and contact thermal resistance components by this method. However, it is difficult to distinguish the intrinsic thermal conductivity from the contact thermal resistance in CNT/SiC composite materials because there are three components (CNT, SiC, and CNT) and four interfaces. We therefore define the practical thermal conductivity k' as follows.

$$k'\ [W/mK] = d/(R_t \cdot A) = (Q \cdot d)/\{(T_h - T_c) \cdot A\} \tag{3}$$

Here, the sample thickness and area are fixed to d = 250 μm and A = 100 mm^2. It should be noted that the practical thermal conductivity k' can be used only in comparing materials having the same thickness and area. It is of particular importance that the practical conductivity k' includes the contact resistance component, in order for the practical conductivity k' to reflect the performance of the actual TIMs directly. The obtained practical thermal conductivities of Si grease, grease with Ag particles, SiC single crystal with grease, SiC single crystal, and 1μm-CNT/SiC single crystal were, respectively, 1.39, 2.13, 4.43, 13.9,

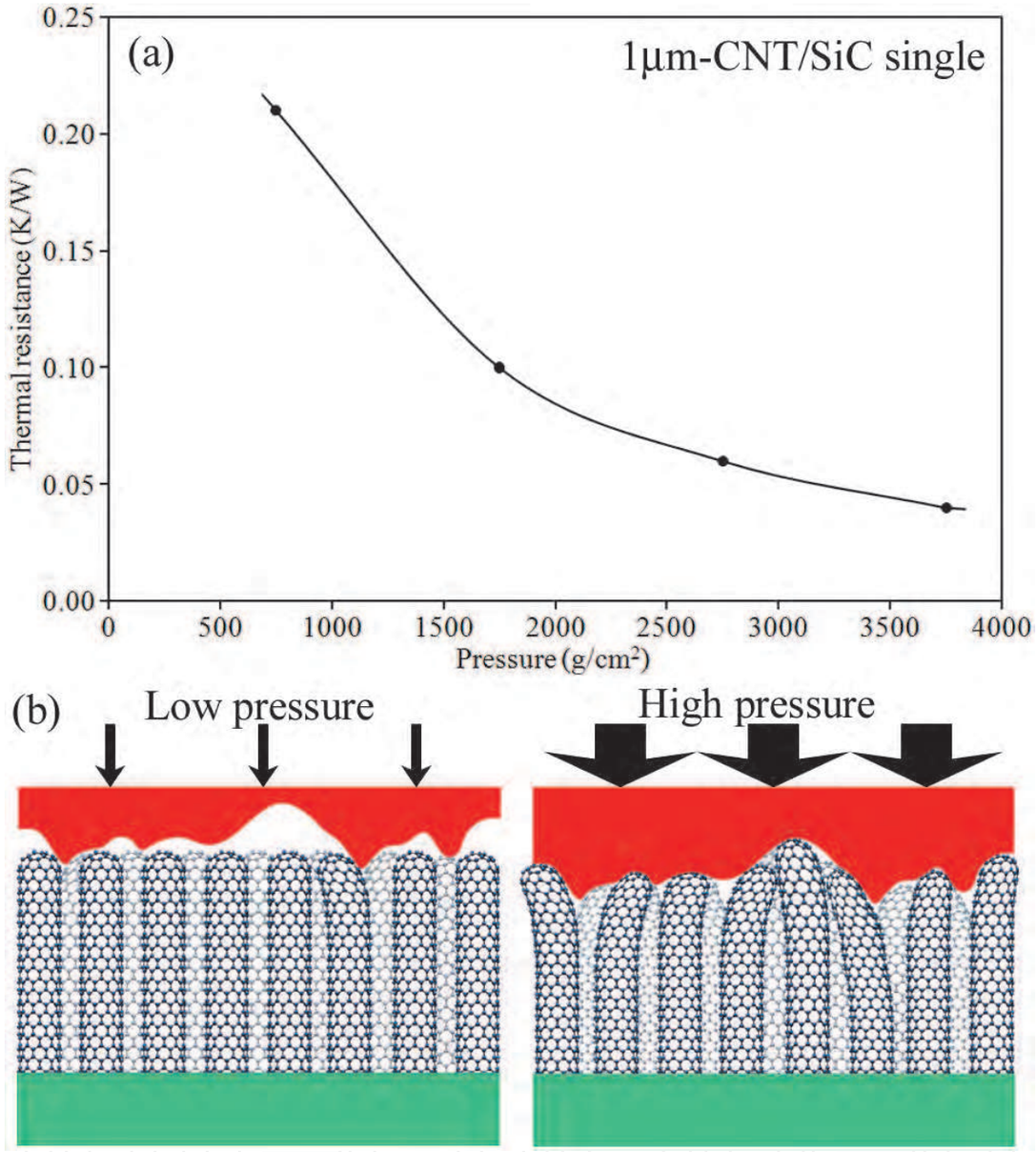

Fig. 6. (a) Pressure dependence of the thermal resistance of the 1μm-CNT/SiC single crystal sample. (b) Schematic diagrams of the contact interface in low pressure and high pressure scenarios.

and 62.5 W/mK. The important item to note here is that the k' value of the SiC single crystal with grease is almost equivalent to that of typically TIMs already in use. The k' value of 1μm-CNT/SiC was then more than 14 times as high as that of a typical TIM. According to published papers, k' values of dispersed-CNT and aligned-CNT were 0.50 and 1.00 W/mK, respectively (Biercuk et al., 2002; Liu et al., 2004: Huang et al., 2005). Our k' value is more than 60 times as high as these. This excellent value is attributed to the extremely dense, and well-aligned CNTs, the flexibility of CNT tips, the high thermal conductivities of CNT and SiC, and the strong adhesion between the CNTs and SiC. The flexible CNT tips and strong

adhesion in the CNT/SiC interface drastically reduce the contact thermal resistance, while the dense CNTs and thermally conductive SiC transport heat quite efficiently. Although a SiC single crystal costs too much for use in a real device, CNT/SiC composites using low-price polycrystalline SiC substrates produced by a CVD method also have sufficiently high thermal conductivities to be effective TIMs.

The above mentioned experimental values were obtained using sample holder (1), of which the surface roughness R_z was 1.0μm and was without the macroscopic surface undulation. Actually, it is not realistic to use the heat sinks with the mirror finished surface due to the high cost performance. In Figures 7 and 8, we show the results using the sample holders of (2) the roughness of R_z = 1.0 μm, and the flatness of ± 0.3 μm, and (3) R_z = 1.0 μm, and the flatness of ± 15 μm, respectively.

In Fig. 7, it is understood that the longer CNTs on the surface of SiC can reduce the contact thermal resistance also for the holders with rough surface. Figure 8 also tells us that CNTs effectively lowers the contact resistance to 0.6 k/W with the rough and undulant contacting surface. However, thermal resistance of about 0.6 K/W is the close value to that of the grease shown in Fig. 5. This is due to the large surface undulation which induces the little contact area and cannot be overcome by CNTs with 4 μm length. In order to increase the contact area, we formed porous graphite region with the thickness of about 60 μm between CNTs and SiC by progressing thermal decomposition of SiC additionally (Kawai et al. 2009). A TEM image of the graphite region is shown in Figure 9.

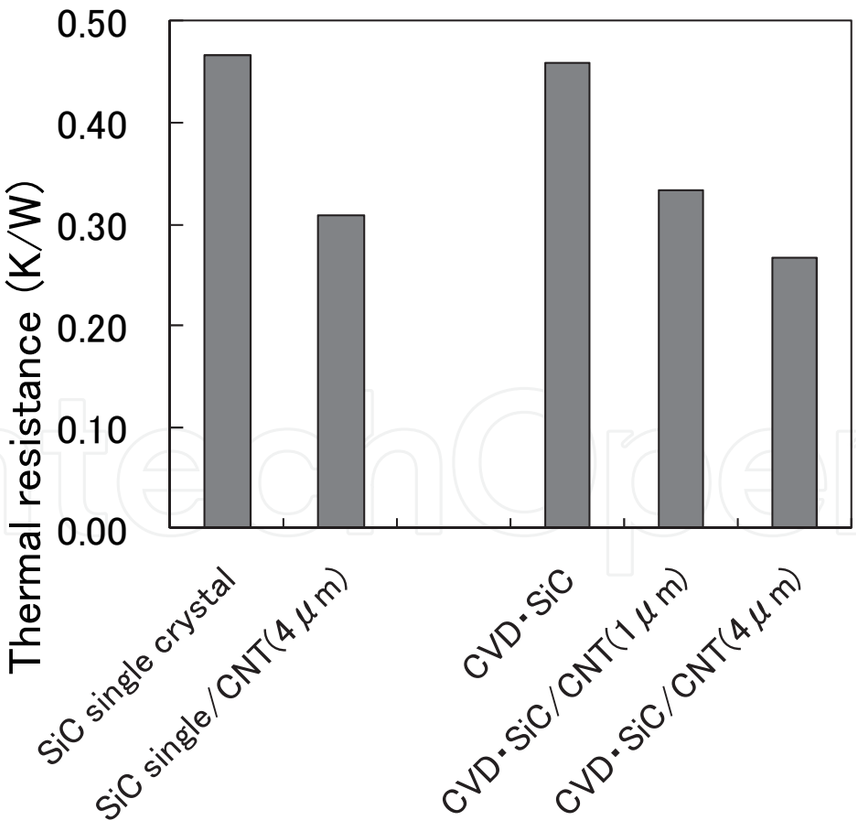

Fig. 7. Thermal resistance of the samples using the sample holders of R_z = 1.0 μm, and the flatness ± 0.3 μm.

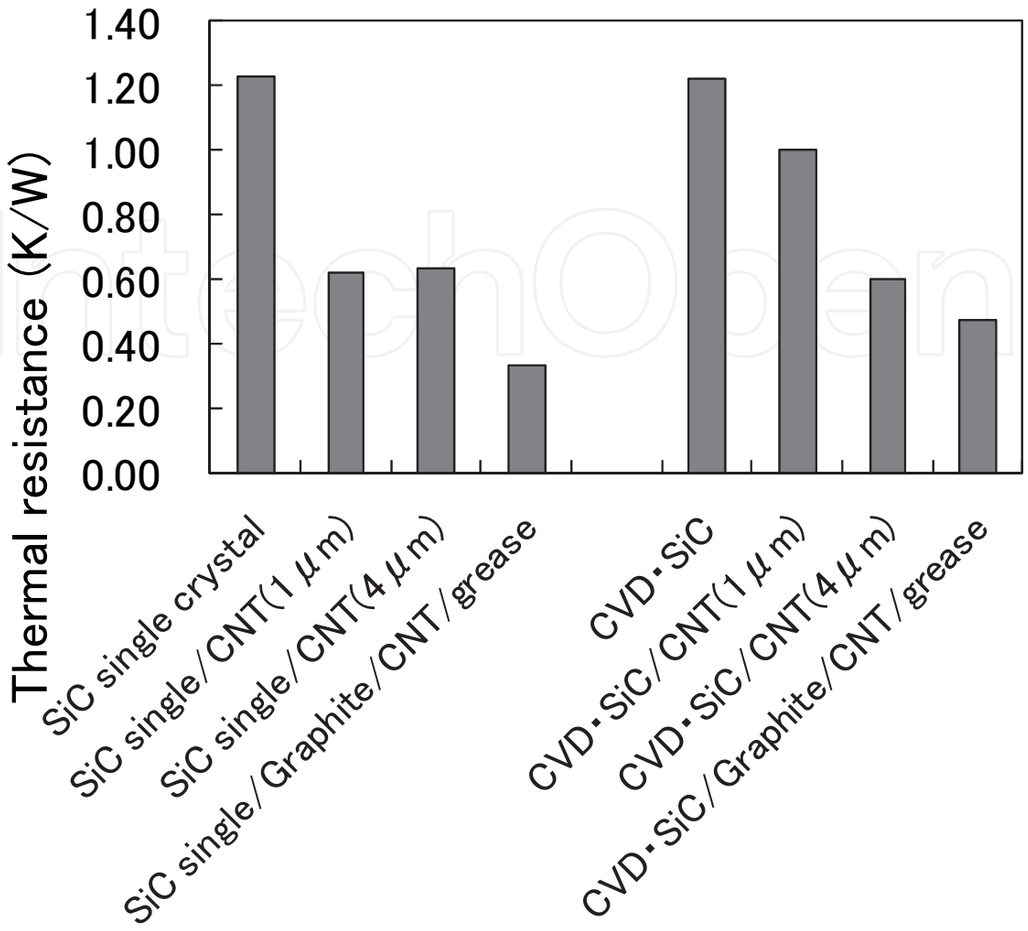

Fig. 8. Thermal resistance of the samples using the sample holders of R_z = 1.0 μm, and the flatness ± 15 μm.

As shown in the image, there are bright area and the plate-like area with the dark contrast. The dark plate-like region consists of the several dozen of graphene layers with the area of several hundred square nanometers, which arrange in the horizontal and the perpendicular directions. These graphite layers surround the hollow area with several hundred square nanometers, indicating the high deformability under pressure. In addition, we used grease together with the sample (Kawai et al., 2009). These results are also shown in Figure 8. The value for SiC single crystal / Graphite / CNT / grease is 0.33 K/W, and 0.47 K/W for CVD-SiC / Graphite / CNT / grease. These favorable values were obtained by the following mechanism, as shown in Figure 10.

The hollow space in graphite can include grease. By applying pressure, highly deformable graphite changes its shape and follows the contacting undulation. In addition to that, grease included in graphite exudes into the interface between CNTs and the contacting material, and helps to increase the contacting area, leading to the decrease in thermal resistance. It is then concluded that the use of CNT / graphite / SiC together with grease can decrease the thermal resistance in the actually used heat-release structure with rough and undulant surface.

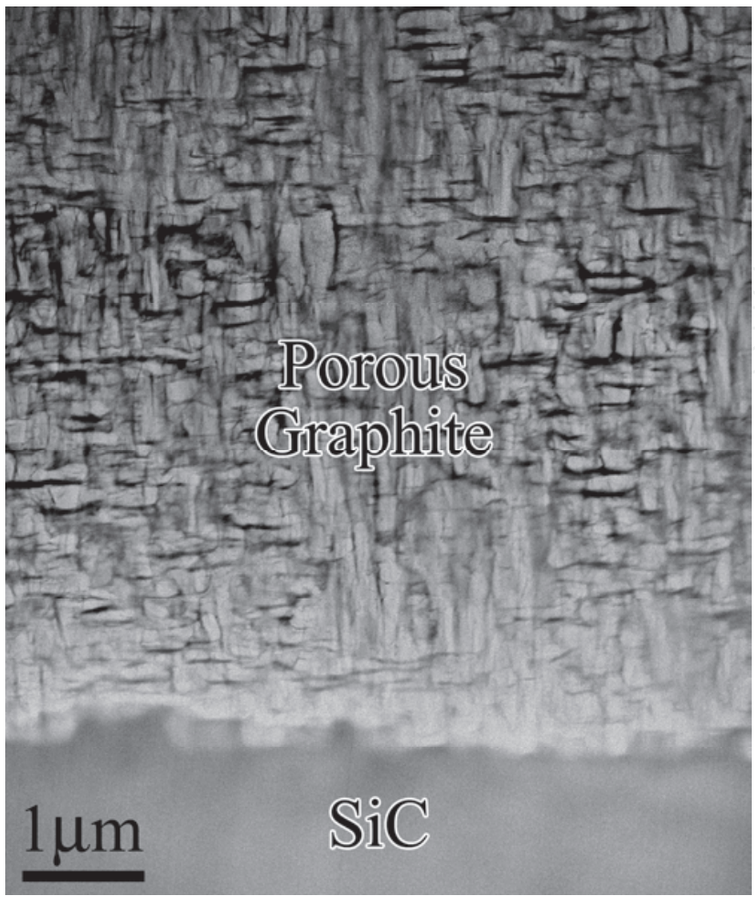

Fig. 9. TEM image of porous graphite formed between CNTs and SiC.

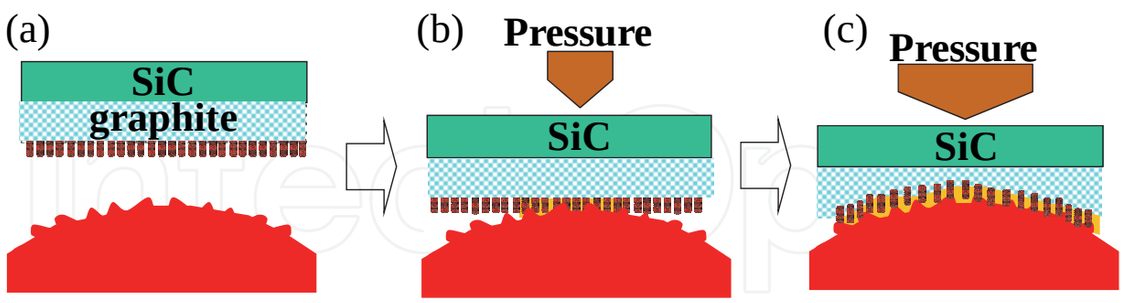

Fig. 10. Schematic diagram of contacting phenomena of CNT / Graphite / SiC with the rough and undulant surface using grease (orange color).

4. Summary

We have demonstrated the excellent performance of CNT/SiC composites as thermal interface materials. There was a more than 14 times enhancement in the practical thermal conductivity with 1μm-CNT/SiC single crystal compared with conventional TIMs. This

high-quality performance results primarily from a combination of the high thermal conductivities of CNT and SiC and the reduction of contact thermal resistance due to the flexibility of the CNT tips. Based on the obtained results, one of the ideal heat-release structures is shown in Figure 11.

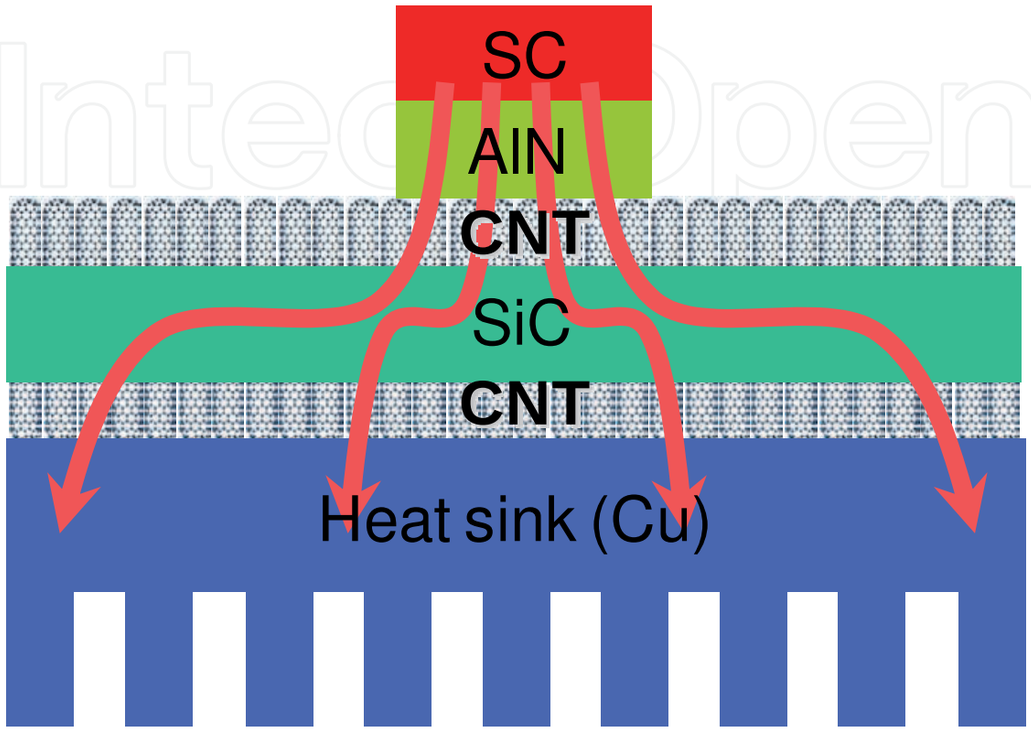

Fig. 11. Possible heat-release structure using the CNT/SiC composite material.

CNT/SiC layered composite materials may be one of the most efficient thermal interface materials which can solve efficiently current serious thermal problems not only in the Si-semiconductor industry, but also in the automobile industry.

5. References

Berber, S., Kwon, Y-K. & Tomanek, D. (2000). *Phys. Rev. Lett.* 84, 4613.

Biercuk, M. J., Llaguno, M. C., Radosavljevic, M., Hyun, J. K., Johnson, A. T. & Fischer, J. E. (2002). *Appl. Phys. Lett.* 80: 2767.

Burgemeister, E. A., von Muench, W. & Pettenpaul, E. (1979). *J. Appl. Phys.* 50: 5790.

Fujii, M., Zhang, X., Xie, H., Ago, H., Takahashi, K., Ikuta, T., Abe, H. & Shimizu, T. (2005). *Phys. Rev. Lett.* 95: 065502.

Huang, H., Liu, C. H., Wu, Y., & Fan, S. S. (2005). *Adv. Mater.* 17: 1652.

Kim, P., Shi, L., Majumdar, A. & McEuen, P. L. (2001). *Phys. Rev. Lett.* 87: 215502.

Kusunoki, M., Rokkaku, M. & Suzuki, T. (1997). *Appl. Phys. Lett.* 71: 2620.

Kusunoki, M., Suzuki, T., Kaneko, K. & Ito, M. (1999). *Phil. Mag. Lett.* 79: 153.

Kusunoki, M., Suzuki, T., Hirayama, T., Shibata, N. & Kaneko, K. (2000). *Appl. Phys. Lett.* 77: 531.

Kusunoki, M., Suzuki, T., Honjo, C., Hirayama, T. & Shibata, N. (2002). *Chem. Phys. Lett.* 366: 458.

Kusunoki, M., Honjo, C. Suzuki, T. & Hirayama, T. (2005). *Appl. Phys. Lett.* 87: 103105.

Lee, C. J., Kim, D. W., Lee, T. J. Choi, Y. C., Park, Y. S., Lee, Y. H., Choi, N. S. Lee, W. B., Park, G-S. & Kim, J. M. (1999). *Chem. Phys. Lett.* 312: 461.

Liu, C. H. , Huang, H., Wu, Y. & Fan, S. S. (2004). *Appl. Phys. Lett.* 84: 4248.

Miyake, K., Kusunoki, M. Usami, H., Umehara, N. & Sasaki, S. (2007). *Nano Lett.* 7: 3285.

Pan, Z. W., Xie, S. S., Chang, B. H., Sun, L. F., Zhou, W. Y. & Wang, G. (1999). *Chem. Phys. Lett.* 299: 97.

PCT/JP2009/004200, Kawai, C., Norimatsu, W. & Kusunoki, M.

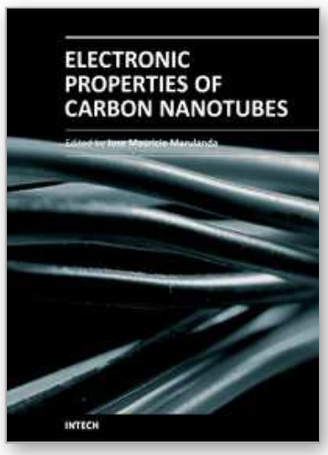

Electronic Properties of Carbon Nanotubes

Edited by Prof. Jose Mauricio Marulanda

ISBN 978-953-307-499-3
Hard cover, 680 pages
Publisher InTech
Published online 27, July, 2011
Published in print edition July, 2011

Carbon nanotubes (CNTs), discovered in 1991, have been a subject of intensive research for a wide range of applications. These one-dimensional (1D) graphene sheets rolled into a tubular form have been the target of many researchers around the world. This book concentrates on the semiconductor physics of carbon nanotubes, it brings unique insight into the phenomena encountered in the electronic structure when operating with carbon nanotubes. This book also presents to reader useful information on the fabrication and applications of these outstanding materials. The main objective of this book is to give in-depth understanding of the physics and electronic structure of carbon nanotubes. Readers of this book should have a strong background on physical electronics and semiconductor device physics. This book first discusses fabrication techniques followed by an analysis on the physical properties of carbon nanotubes, including density of states and electronic structures. Ultimately, the book pursues a significant amount of work in the industry applications of carbon nanotubes.

InTech Europe
University Campus STeP Ri
Slavka Krautzeka 83/A
51000 Rijeka, Croatia
Phone: +385 (51) 770 447
Fax: +385 (51) 686 166
www.intechopen.com

InTech China
Unit 405, Office Block, Hotel Equatorial Shanghai
No.65, Yan An Road (West), Shanghai, 200040, China
中国上海市延安西路65号上海国际贵都大饭店办公楼405单元
Phone: +86-21-62489820
Fax: +86-21-62489821

IntechOpen